

NFATc3 Mediates Chronic Hypoxia-induced Pulmonary Arterial Remodeling with α -Actin Up-regulation*

Received for publication, March 28, 2007. Published, JBC Papers in Press, April 2, 2007, DOI 10.1074/jbc.M702679200

Sergio de Frutos, Rhyannon Spangler, Dominique Alò, and Laura V. González Bosc¹

From the Department of Cell Biology and Physiology, School of Medicine, University of New Mexico, Albuquerque, New Mexico 87131

Physiological responses to chronic hypoxia include polycythemia, pulmonary arterial remodeling, and vasoconstriction. Chronic hypoxia causes pulmonary arterial hypertension leading to right ventricular hypertrophy and heart failure. During pulmonary hypertension, pulmonary arteries exhibit increased expression of smooth muscle- α -actin and -myosin heavy chain. NFATc3 (nuclear factor of activated T cells isoform c3), which is a Ca^{2+} -dependent transcription factor, has been recently linked to smooth muscle phenotypic maintenance through the regulation of the expression of α -actin. The aim of this study was to determine if: (a) NFATc3 is expressed in murine pulmonary arteries, (b) hypoxia induces NFAT activation, (c) NFATc3 mediates the up-regulation of α -actin during chronic hypoxia, and (d) NFATc3 is involved in chronic hypoxia-induced pulmonary vascular remodeling. NFATc3 transcript and protein were found in pulmonary arteries. NFAT-luciferase reporter mice were exposed to normoxia (630 torr) or hypoxia (380 torr) for 2, 7, or 21 days. Exposure to hypoxia elicited a significant increase in luciferase activity and pulmonary arterial smooth muscle nuclear NFATc3 localization, demonstrating NFAT activation. Hypoxia induced up-regulation of α -actin and was prevented by the calcineurin/NFAT inhibitor, cyclosporin A (25 mg/kg/day s.c.). In addition, NFATc3 knock-out mice did not show increased α -actin levels and arterial wall thickness after hypoxia. These results strongly suggest that NFATc3 plays a role in the chronic hypoxia-induced vascular changes that underlie pulmonary hypertension.

As altitude increases, the barometric pressure and atmospheric oxygen partial pressure decrease. This decrease in barometric pressure is the basic cause of all hypoxia-related problems in high altitude pathophysiology. Similar levels of hypoxia are present in patients with chronic bronchitis, emphysema, cystic fibrosis, asthma, and severe restrictive lung diseases (1). Chronic hypoxia (CH)² causes pulmonary hypertension due to

pulmonary vasoconstriction, arterial remodeling, and polycythemia, which ultimately results in right ventricular (RV) hypertrophy and often heart failure (2).

Pulmonary vasoconstriction is thought to be caused by elevated vascular tone through increased pulmonary arterial smooth muscle cell (PASMC) intracellular Ca^{2+} ($[\text{Ca}^{2+}]_i$) (3–8) and increased sensitivity of the contractile apparatus to Ca^{2+} (9–12).

Regardless of the cause of pulmonary hypertension, the structural change that is thought to underlie the increased vascular resistance is remodeling of small pulmonary arteries. A prominent feature of this vascular remodeling is medial thickening. In proximal pulmonary vessels, medial enlargement is caused by hypertrophy and hyperplasia of the pre-existing smooth muscle cells (reviewed in Ref. 1). In addition, differentiation of adventitial fibroblasts into myofibroblasts contributes to medial thickening (13).

Smooth muscle is phenotypically dynamic and maintains its differentiated phenotype through the regulated expression of a repertoire of SM-specific genes (reviewed in Ref. 14–17). NFAT (nuclear factor of activated T cells), a Ca^{2+} -dependent transcription factor that regulates the expression of genes in both immune and non-immune cells (18, 19), has been recently linked to smooth muscle phenotypic maintenance (20–25). NFAT appears to regulate the expression of SM-myosin heavy chain, SM- α -actin, $\alpha 1$ integrin, and caldesmon genes (21, 22). Recently, we demonstrated that serum response factor (SRF) and NFATc3 cooperatively enhance the expression of SM- α -actin in cultured aortic smooth muscle cells (24). NFATc3 and SRF bind to a region of the first intron of the SM- α -actin gene (24).

SM- α -actin is required for the high force development properties of smooth muscle cells and is the most abundant protein in differentiated SM making up to 40% of total cell protein (26). In adults, expression of SM- α -actin is restricted and is generally activated upon terminal differentiation in cells of myogenic lineage correlating with hypertrophy, whereas increases in non-muscle actins (β - and γ -actin) coincide with cell growth and proliferation (14).

The NFAT family consists of four members (NFATc1, NFATc2, NFATc3, NFATc4) that share the property of Ca^{2+} /calcineurin-dependent nuclear translocation, and a fifth mem-

* This work was supported in part by Dedicated Health Research Funds of the UNM SOM and a Postdoctoral Fellowship from Ministerio de Educación y Ciencia, Spain (to S. D. F.). The costs of publication of this article were defrayed in part by the payment of page charges. This article must therefore be hereby marked "advertisement" in accordance with 18 U.S.C. Section 1734 solely to indicate this fact.

¹ To whom correspondence should be addressed: Dept. of Cell Biology and Physiology, School of Medicine, University of New Mexico, MSC 08 4750, Albuquerque, NM 87131. Tel.: 505-272-0605; Fax: 505-272-9105; E-mail: lgonzalezbosc@salud.unm.edu.

² The abbreviations used are: CH, chronic hypoxia; PASMC, pulmonary arterial smooth muscle cells; $[\text{Ca}^{2+}]_i$, intracellular Ca^{2+} concentration; SM, smooth muscle; NFAT, nuclear factor of activated T cells; SRF, serum response factor; VSMC, vascular smooth muscle cells; Ang II, angiotensin II; NFAT-luc,

9xNFAT-luciferase mice; NFATc3 KO, NFATc3 knockout mice; WT, wild type mice; CsA, cyclosporin A; qRT-PCR, quantitative real-time polymerase chain reaction; ET-1, endothelin 1; K_v channels, voltage-dependent K channels; E_m , membrane potential; T, total ventricle weight; RV, right ventricular.

NFATc3 Regulates α -Actin Expression

ber, NFAT5, which is Ca^{2+} independent and shares limited homology with the other family members (reviewed in Refs. 19, 27, 28).

The NFATc3 isoform is specifically implicated in vasculature development (20, 25), maintenance of a contractile phenotype (24) and regulation of vascular smooth muscle cell (VSMC) contractility (29).

In smooth muscle, NFAT is activated by $G_q/11$ -coupled receptor agonists, such as uridine triphosphate, endothelin 1 (ET-1) and angiotensin II (Ang II) (23, 30–32). This activation is mediated by calcineurin and is dependent on both sarcoplasmic reticulum Ca^{2+} release through inositol trisphosphate receptors (IP_3R) and extracellular Ca^{2+} influx through voltage-dependent Ca^{2+} channels (VDCC) (31).

Interestingly, during CH, PSMC exhibit increased expression of SM- α -actin (33, 34) consistent with PSMC hypertrophy and vascular remodeling (35). In addition, it has been shown that Ang II, which is elevated during CH (36–38), induces stimulation of SM- α -actin expression at the transcriptional level through a SRF-dependent mechanism in cultured VSMC (36–39). It is thus reasonable to hypothesize that in response to CH, NFAT is activated in PSMC leading to the up-regulation of the SM- α -actin contractile protein and vascular remodeling.

Given the lack of evidence demonstrating hypoxia-induced NFAT regulation of gene transcription, the aims of the present study were to determine if: (a) NFATc3 is expressed in murine pulmonary arteries, (b) CH induces NFATc3 activation, (c) NFATc3 mediates the up-regulation of α -actin during CH, and (d) NFATc3 is involved in CH-induced pulmonary vascular remodeling.

In support of this hypothesis, our data demonstrate that CH indeed increases NFAT transcriptional activity and NFATc3 nuclear translocation in mouse pulmonary arteries. Furthermore, pharmacological inhibition of calcineurin activation of NFAT or genetic ablation of NFATc3 prevents CH-induced increases in α -actin expression, arterial wall thickness and right ventricular (RV) hypertrophy. These results suggest that NFATc3 plays a role in the vascular changes observed during CH-induced pulmonary hypertension.

EXPERIMENTAL PROCEDURES

All protocols employed in this study were reviewed and approved by the Institutional Animal Care and Use Committee of the University of New Mexico, School of Medicine (Albuquerque, NM).

Animals—Adult male 9x-NFAT-luciferase reporter (NFAT-luc), NFATc3 knock-out (NFATc3 KO), Balb/C wild-type (WT) and C57BL/6 (Harland Laboratories) mice (20–25 g) were used. In addition, NFAT-luc were backcrossed with NFATc3 KO for, at least, two generations and NFAT-luc/NFATc3 +/+ (WT), NFAT-luc/NFATc3 +/- (HET), and NFAT-luc/NFATc3 -/- (KO) were used. NFAT-luc mice have been provided by Dr. Jeffery D. Molckentin (Department of Pediatrics, Children's Hospital Medical Center, Cincinnati, OH) (40). NFATc3 KO mice have been kindly provided by Dr. Laurie Glimcher (Harvard University) (41). Heterozygous mice were bred to obtain age-matched WT (Balb/C) and KO. Importantly,

it has been shown that the loss of NFATc3 isoform does not induce a compensatory regulation of other NFAT isoforms (42). C57B6 mice were s.c. administered 25 mg/kg/day of cyclosporin A (CsA, Calbiochem) or Cremophor EL (vehicle) for 1 week.

Chronic Hypoxia Exposure—Animals designated for exposure to CH were housed in a hypobaric chamber with barometric pressure maintained at ~ 380 mmHg for 2, 7, or 21 days. The chamber was opened one time per week to provide animals with fresh food, water, and clean bedding. Control animals were housed at ambient barometric pressure (Normoxia, N, ~ 630 mmHg). All animals were maintained on a 12:12-h light-dark cycle.

Assessment of Polycythemia and RV Hypertrophy—Blood samples were obtained by direct cardiac puncture at the time of lung isolation for measurement of hematocrit. RV hypertrophy was assessed as an index of CH-induced pulmonary hypertension with previously described methods (43, 44). Briefly, after isolation of the heart, the atria and major vessels were removed from the ventricles. The RV was dissected from the left ventricle and septum, and each was weighed. The degree of RV hypertrophy was expressed as the ratio of RV to total ventricle weight (T).

Vascular Morphometry—Animals were anesthetized with 5% isoflurane in O_2 and perfused via the left ventricle with ~ 20 ml of modified physiological saline solution (HEPES-PSS, 134 mM NaCl, 6 mM KCl, 1 mM MgCl, 10 mM HEPES, 2 mM CaCl_2 , 0.026 mM EDTA, and 10 mM glucose) containing heparin, 4% albumin (Sigma) and 10^{-4} M papaverine (Sigma), at a rate close to normal cardiac output in mice (17 ml/minute) to maximally dilate and flush the circulation of blood. Then, mice were perfused with 4% formaldehyde (Polyscience) and 10^{-4} M papaverine (Sigma) in PBS at the same rate. Following fixation, the lungs were inflated via the trachea to a pressure of 23 cmH₂O with fixative. The tissue was then dehydrated in increasing concentrations of ethanol, with a final dehydration in xylene, and then embedded in paraffin. Lung sections (5 μm) were stained with hematoxylin/iodine/eosin (Van Gieson staining, Sigma) which stains nuclei, elastic laminae, collagen fibers and cellular cytosol to distinguish arteries from veins. A total of 1291 arteries from 13 mice were analyzed. Vessels were examined with a $\times 40$ objective on a Nikon Diaphot 300 microscope, and images were generated with a cooled digital CCD camera (Photometrics SenSys 1400). Vessel images were processed with Metamorph imaging system hardware and software (Universal Imaging). Vessels sectioned at oblique angles were excluded from analysis. Media and wall thickness were measured and compared between groups using the following equation: Wall thickness (%) = $\frac{\text{perimeter}_{\text{ext}} - \text{perimeter}_{\text{int}}}{\text{perimeter}_{\text{ext}}} \times 100$, where $\text{perimeter}_{\text{ext}}$ and $\text{perimeter}_{\text{int}}$ are the circumferences bounded by external and internal elastic laminae, respectively (45).

Luciferase Activity—NFAT-luc mice were euthanized with an overdose of pentobarbital solution (200 mg/kg intraperitoneal). Following euthanasia lungs, brain, and small intestines were removed and placed into ice-cold HEPES-PSS. Aorta, intrapulmonary, cerebral and mesenteric arteries were isolated and lysed using tissue lysis buffer from Promega according to manufacturer's protocol. Lysate was centrifuged for 10 min at

10,000 rcf. Both luciferase activity and protein content were determined in the supernatant. Luciferase activity was measured using a Luciferase Assay System kit (Promega), and light detected with a luminometer (TD20/20, Turner). Protein content was determined by the Bradford method (Bio-Rad) and used to normalize luciferase activity per sample.

Immunofluorescence Confocal Microscopy—Isolated lungs were formaldehyde fixed (4% in PBS), cryoprotected with 30% sucrose in PBS, embedded in OCT media and frozen. Cryostat sections (10 μ m) were permeabilized and blocked for nonspecific binding, primary antibodies (rabbit polyclonal anti-NFATc3 (1:100); Santa Cruz Biotechnology and anti- α -actin (1:250); Sigma) were prepared in 0.2% gelatin in PBS and applied overnight at 4 °C. Secondary antibodies (anti-rabbit Cy5 and anti-mouse Cy3 (1:500); Jackson ImmunoResearch Laboratories) were prepared in 0.2% gelatin in PBS and applied for 1 h at room temperature. Nuclei were stained using SYTOX green (1:5,000 in PBS; Molecular Probes). Sections were examined using a 40 \times objective on a Zeiss 510 laser scanning confocal microscope. Specificity of immune staining was confirmed by the absence of fluorescence in tissues incubated with primary or secondary antibodies alone. For scoring of NFATc3-positive nuclei, multiple fields for each vessel were imaged and counted by two independent observers using Metamorph software (Universal Imaging Corp). The software was programmed so that individual pixels appear white instead of yellow if the green nucleic acid stain and red NFATc3 stain co-localized. Thus, a cell was considered positive if co-localization (white) was uniformly distributed in the nucleus and negative if no co-localization (green only) was observed.

Western Blot Analysis—Isolated intrapulmonary arteries were homogenized in lysis buffer (10 mM Tris-HCl pH 7.4, 1 mM EDTA, 1% IGEPAL, 0.1% sodium deoxycholate, 500 nM sodium orthovanadate, 50 nM NaF, 1 μ g/ml pepstatin/leupeptin/aprotinin, 1 mM phenylmethylsulfonyl fluoride) at 4 °C, and centrifuged at 16,000 rcf for 2 min. Protein concentration was determined in the supernatant using Bradford's method (Bio-Rad) as recommended by the manufacturer. To perform Western blot analysis, supernatants (2 μ g/lane) were resolved by SDS-PAGE and proteins transferred to polyvinylidene difluoride membranes. The membranes were blocked with Tris-buffered (50 mM) saline solution (pH 7.6) with 0.05% Tween containing 5% milk powder at room temperature for 1 h. The membranes were incubated with primary anti SM- α -actin antibody (1:5000, Sigma) or anti β -actin antibody (1:5000) at 4 °C overnight, washed, and incubated with a peroxidase-conjugated secondary antibody (Pierce) for 1 h at room temperature. Specifically bound antibody was detected by enhanced chemiluminescence detection (ECL, Pierce). Relative content of the antigen protein was evaluated using a Gene Gnome imaging system and Genesnap software (Syngene, Cambridge, UK). Band densities were normalized to total protein loaded per lane as determined by Coomassie Blue or Sypro Red II staining of the membrane (NIH Image software).

Quantitative Real-time Polymerase Chain Reaction (qRT-PCR)—Intrapulmonary arteries were stored in RNAlater (Ambion). Total RNA was isolated using the RNeasy Mini kit (Qiagen) following the manufacturer's protocol, with the addi-

tional steps of DNase treatment (DNase turbo from Ambion) and RNeasy MinElute Cleanup kit (Qiagen) to remove possible genomic DNA contamination. Total RNA was reverse-transcribed to cDNA using TaqMan Reverse Transcription kit (A&B). For real time detection of SM- α -actin transcripts (Mm01546133_mi) and reference gene (18S, 4319413E-0502018), TaqMan Gene Expression Assays (A&B) were used. PCR was performed using Applied Biosystems 7500 Fast Real-Time PCR System. The normalized gene expression method ($2^{-\Delta\Delta CT}$) for relative quantification of gene expression was used (46).

Qualitative RT-PCR—Total RNA from intrapulmonary arteries (isolated as mentioned above) was reverse-transcribed (iScript, cDNA synthesis Kit, Bio-Rad). PCR was performed using the iTaq DNA polymerase (Bio-Rad) with the following sets of primer pairs: for NFATc3, 5'-CTACTGGTGGCCATCCTGTTGT-3' and 5'-AGCTCGTGGGCAGAGCGCTGAGAGCACTC-3'; and for cyclophilin, 5'-CAGACAAAGTTCCAAAGACA-3' and 5'-AGTTCGACCGTCTTCTCAGC-3'. Amplification conditions were 94 °C for 10 min, 45 cycles at 94 °C for 1 min, 55 °C for 1 min, 72 °C for 2 min, and extension for 10 min at 72 °C. Amplified PCR products were separated by agarose gel electrophoresis and detected by ethidium bromide staining.

Statistical Analysis—Data were expressed as mean \pm S.E. Statistical significance was tested at 95% ($p < 0.05$) confidence level using unpaired Student's *t* test, one-way analysis of variance (ANOVA) followed by Newman-Keuls multiple comparisons test or two-way ANOVA followed by the Bonferroni multiple comparisons test.

RESULTS

NFATc3 Isoform Is Expressed in Mouse Pulmonary Arteries—We have used RT-PCR analysis, immunoblotting and immunofluorescence confocal microscopy to identify NFATc3 expression in native pulmonary arteries isolated from mice. We found transcripts for NFATc3 (Fig. 1A) and protein by Western blot (Fig. 1B). NFATc3 immunofluorescence staining was mainly localized in PASM (3A).

CH Increases NFAT Activity and NFATc3 Nuclear Accumulation in Pulmonary Arteries—Most of the mediators of NFAT activation are up-regulated during CH, including PASM [Ca²⁺]_i, Ang II (36–38), and endothelin 1 (ET-1) (4;6–8;47;48), although there are no reports of hypoxic activation of NFAT either *in vivo* or *in vitro*. Therefore, we examined the effect of different exposure times to CH on NFAT activity in tissues from NFAT-luc reporter mice. We found that CH elicited a significant increase in luciferase activity in pulmonary arteries (Fig. 2A). Interestingly, although luciferase activity decreased in a time dependent manner, it remained significantly elevated over normoxic values even at day 21. No increase in activity was observed in any of the other tissues studied (data not shown). These results for the first time demonstrate that NFAT is activated by CH in pulmonary arteries, suggesting that it is an early response transcription factor under these conditions.

Because NFATc3 is expressed in PASM, we sought to establish the contribution of NFATc3 to CH-increased NFAT activity. Therefore, we determined the effect of 2 days of

NFATc3 Regulates α -Actin Expression

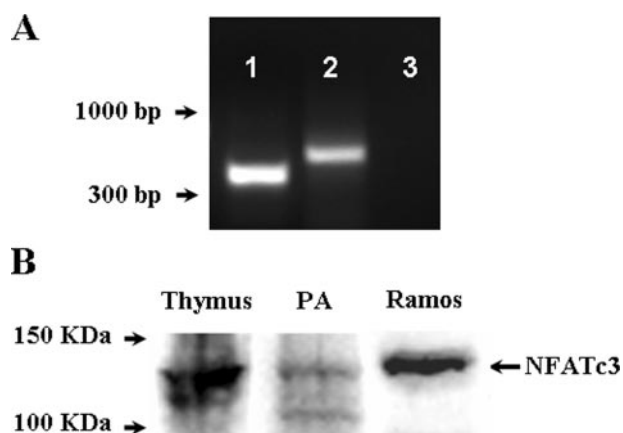


FIGURE 1. NFATc3 is expressed in mouse pulmonary arteries. *A*, RT-PCR analysis of NFATc3 expression in isolated intrapulmonary arteries from 9xNFAT-luc mice. Lane 1 shows amplification of NFATc3. Amplification of cyclophilin (control) from pulmonary arteries is shown in lane 2. Lane 3 corresponds to a control without the reverse transcription step. The experiment was repeated at least three times and the same bands were detected in pulmonary arteries from all the mouse strains used in this study. *B*, Western analysis of NFATc3 protein expression in thymus (C57Bl6), pulmonary arteries (9xNFAT-luc), and human Burkitt's lymphoma-derived Ramos cells. Thymus and Ramos cells were used as positive control.

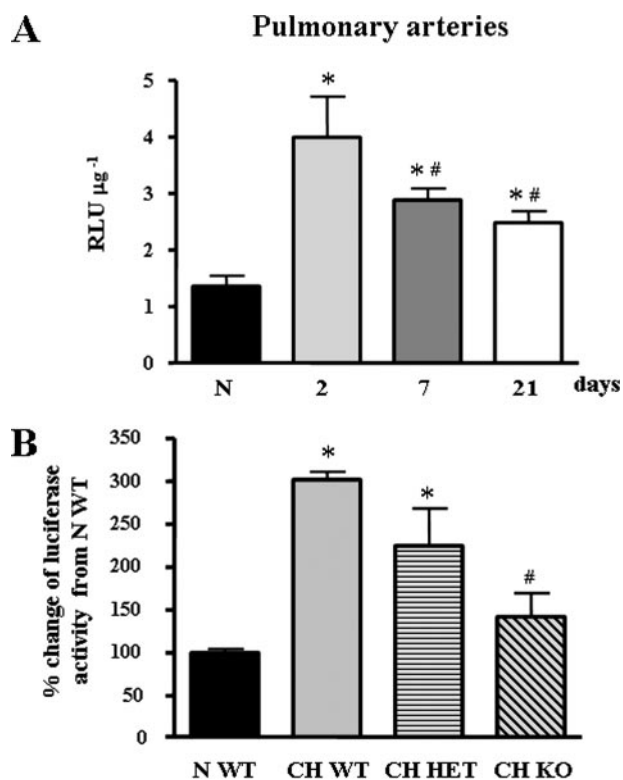


FIGURE 2. NFAT is activated by CH in pulmonary arteries. *A*, pulmonary arteries were isolated from 9xNFAT-luc mice exposed to normoxia (N), or to 2, 7, or 21 days of CH. RLU μg^{-1} = luciferase activity normalized by μg of total protein. *, $p < 0.05$ versus N; #, $p < 0.05$ versus 2 days, $n = 5$ animals. *B*, pulmonary arteries were isolated from 9xNFAT-luc/NFATc3 WT, HET, and KO mice exposed to 2 days of CH. Luciferase activity was normalized by μg of total protein and expressed as percent change from N WT (average = 1.36 ± 0.19). *, $p < 0.01$ versus N WT; #, $p < 0.05$ versus CH WT and HET, $n = 4-8$ animals.

hypoxia on reporter expression in pulmonary arteries isolated from NFAT-luc/NFATc3 WT, NFAT-luc/NFATc3 HET, and NFAT-luc/NFATc3 KO mice. Consistent with the demon-

strated expression of NFATc3 in pulmonary arteries (Figs. 1, *A* and *B*, and 3*A*) and the significant contribution of this isoform to SMC function (23, 24, 29), we found that the reporter response to hypoxia was significantly impaired in pulmonary arteries isolated from NFAT-luc/NFATc3 KO mice (Fig. 2*B*). As expected, HET arteries displayed an intermediate phenotype. The reporter activity in NFAT-luc/NFATc3 WT arteries after 2 days of hypoxia was similar to the values obtained in CH NFAT-luc arteries (3.03 ± 0.82 versus 4.62 ± 0.84). Furthermore, the values obtained in the NFAT-luc/NFATc3 KO arteries were similar to the luciferase activity in both NFAT-luc and NFAT-luc/NFATc3 WT arteries under normoxia. These results demonstrate that NFATc3 significantly contributes to CH-induced NFAT transcriptional activity.

Consistent with the luciferase activity data, PASMC NFATc3 nuclear accumulation increased significantly at every time point of hypoxia exposure (Fig. 3, *A* and *B*). However, the highest value of NFAT activity was at day 2 whereas NFATc3 nuclear accumulation was at day 7. Administration of CsA significantly attenuated the CH-induced increase in NFATc3 nuclear accumulation in PASMC (Fig. 3*C*). In addition, it reduced basal NFATc3 nuclear localization. CsA is an immunosuppressant that inhibits calcineurin, the Ca^{2+} /calmodulin-dependent phosphatase that dephosphorylates NFAT allowing its nuclear import (19).

Calcineurin/NFAT Inhibition with CsA and Genetic Deletion of the NFATc3 Isoform Prevent CH-induced RV Hypertrophy but Not Polycythemia—RV hypertrophy is a consequence of increased pulmonary arterial pressure and is used as an index of pulmonary hypertension (2). To assess CH induced RV hypertrophy, we determined the change of RV/T weight as a % of normoxic control values. RV hypertrophy was determined in vehicle and CsA-treated C57B6 male mice exposed to 1 week of hypobaric CH or normoxia. Greater RV/T ratios were observed for CH vehicle-treated mice compared with normoxic controls (Fig. 4*A*), thus demonstrating RV hypertrophy indicative of pulmonary hypertension. Interestingly, CsA treatment attenuated CH-induced RV hypertrophy (Fig. 4*A*).

Because calcineurin can dephosphorylate other cellular proteins (19) and NFATc3 is the isoform that is activated by CH (Fig. 2*B*), we determined changes in RV/T weight in WT and NFATc3 KO exposed to 3 weeks CH or normoxia. As expected, CH induced RV hypertrophy in WT mice, whereas in the KO the hypertrophic response was significantly attenuated (Fig. 4*A*). These findings suggest that NFATc3 contributes to the development of pulmonary arterial hypertension.

In addition, CH mice exhibited polycythemia as evidenced by a significantly greater hematocrit compared with normoxic animals (Fig. 4*B*). This polycythemic response was similar in vehicle- and CsA-treated and in WT and KO CH mice, demonstrating that NFATc3 is not involved in the polycythemic response to CH.

Calcineurin/NFAT Inhibition with CsA and Genetic Deletion of the NFATc3 Isoform Prevent CH-induced Increases in Expression of SM- α -actin in Pulmonary Arteries—It has been previously demonstrated that CH increases the expression of contractile proteins, such as SM- α -actin, and it mediates PASMC hypertrophy (33). NFATc3 regulates SM- α -actin expression in

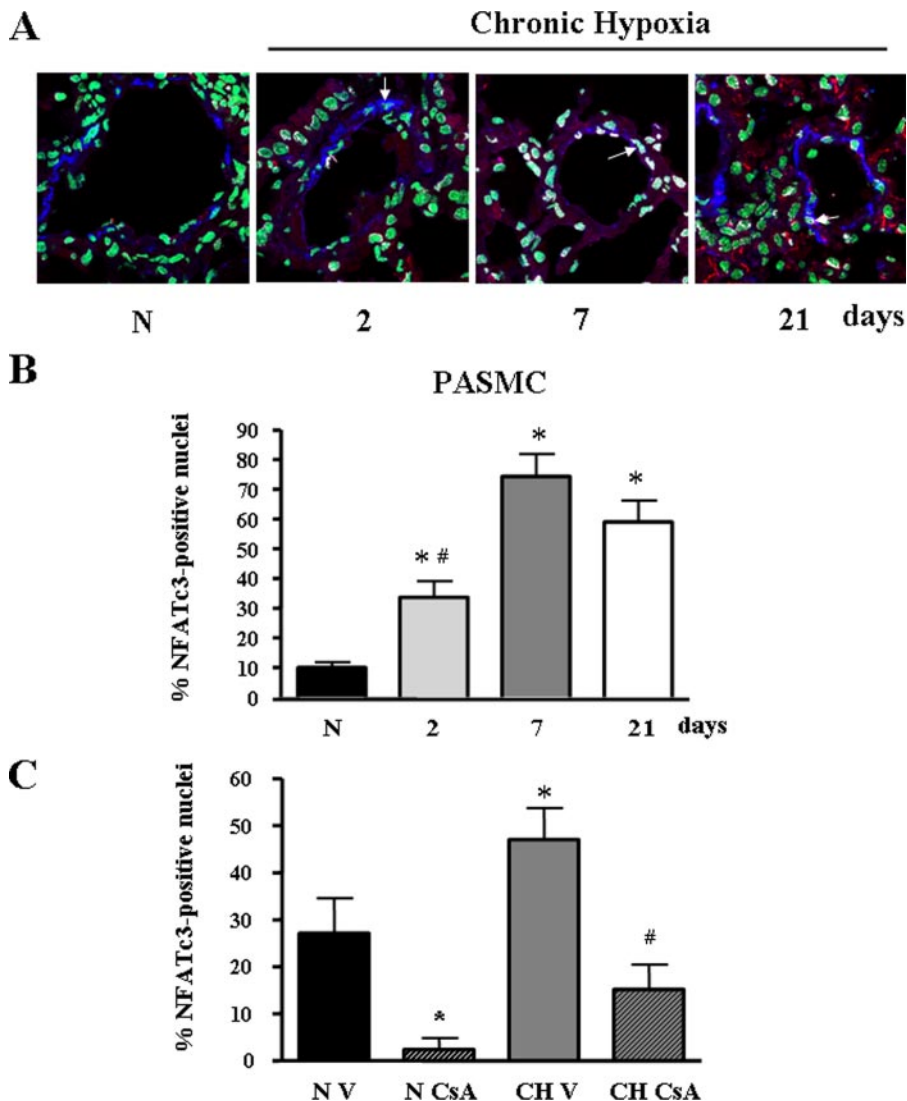


FIGURE 3. NFATc3 nuclear accumulation increases in pulmonary arterial smooth muscle cells after CH. A, representative images showing cytosolic localization of NFATc3 under normoxic (N) conditions and nuclear localization following exposure to CH for 2, 7, or 21 days. Lung sections from 9xNFAT-luc mice were co-stained with the DNA-binding dye SYTOX (green), anti-NFATc3 (red) and anti-SM- α -actin (blue). Pulmonary arterial smooth muscle nuclear co-localization of NFATc3 is shown in white. Arrows indicate examples of NFATc3 positive nuclei. B, summary of effects of CH on NFATc3 nuclear accumulation over time. *, $p < 0.05$ versus N; #, $p < 0.05$ versus 7 and 21 days, $n = 14$ images from at least 3 animals/group (4 arteries/animal). C, summary of effects of CsA on CH-induced NFATc3 nuclear accumulation. C57B6 mice were treated with vehicle (V) or CsA (25 mg/kg/day) and exposed to N or 7 days of CH. Lung sections were stained as in A. *, $p < 0.05$ versus N V; #, $p < 0.05$ versus CH V, $n = 6$ images from at least 3 animals/group (2 arteries/animal).

aortic smooth muscle cells in culture by binding to the intronic region of its promoter (24). To determine if NFAT mediates SM- α -actin up-regulation during CH *in vivo*, we measured SM- α -actin transcript and protein levels in intrapulmonary arteries isolated from vehicle and CsA-treated C57B6 male mice exposed to 1 week hypobaric CH or normoxia. SM- α -actin transcript (real-time PCR) and protein levels (Western blot) significantly increased after 1 week of CH. NFAT inhibition with CsA completely prevented this response (Fig. 5, A and B), suggesting that CH-induced activation of NFAT in pulmonary arteries mediates SM- α -actin up-regulation.

Because calcineurin NFATc3 is the isoform demonstrated to regulate SM- α -actin (24), we evaluated SM- α -actin protein levels (immunoblot) in NFATc3 KO and WT littermates exposed

to hypoxia. In contrast to the effect of 1 week CH exposure on α -actin expression in C57BC mice (Fig. 5), a similar period of hypoxic acclimation did not alter α -actin protein levels in NFATc3 WT BalB/C mice (data not shown). However, after 3 weeks of CH, SM- α -actin protein levels significantly increased in pulmonary arteries from CH WT mice, whereas no changes were observed in arteries from CH NFATc3 KO (Fig. 6A). Although the response time appears to be different in BalB/C and C57B6 mice, these findings clearly demonstrate that NFATc3 mediates up-regulation of SM- α -actin during CH. Together with the CsA experiments, these results further demonstrate that CH-induced up-regulation of SM- α -actin is mediated by calcineurin activation.

Neither CH nor Genetic Deletion of NFATc3 Isoform Affects Expression of β -Actin in Pulmonary Arteries—To confirm that NFATc3 is specifically regulating the expression of SM- α -actin during CH and that the effects seen are not simply due to an overall increase in protein synthesis associated with pulmonary arterial remodeling, we determined β -actin protein levels in pulmonary arteries from WT and NFATc3 KO exposed to 3 weeks of CH. β -actin protein levels did not change in any of the groups (Fig. 6B). These results demonstrate that the effect of CH is specific to the contractile protein α -actin and not to the related cytoskeletal protein β -actin.

Genetic Deletion of NFATc3 Isoform Prevents CH-induced Increases

in Arterial Wall Thickness—The structural changes that are thought to underlie the increased vascular resistance during CH include remodeling of small pulmonary arteries. A prominent feature of vascular remodeling is medial thickening (1) (Fig. 7). In proximal pulmonary vessels, medial enlargement is caused by hypertrophy and hyperplasia of the pre-existing smooth muscle cells whereas distal arteries that were previously non-muscularized become muscularized (1). Our data suggest that NFATc3 is involved in CH-induced pulmonary arterial remodeling because CH-increased α -actin expression in pulmonary arteries, a marker of smooth muscle differentiation and hypertrophy (17), was prevented by inhibiting calcineurin/NFATc3. To further address this possibility, changes in pulmonary arterial wall thickness were evaluated in WT and

NFATc3 Regulates α -Actin Expression

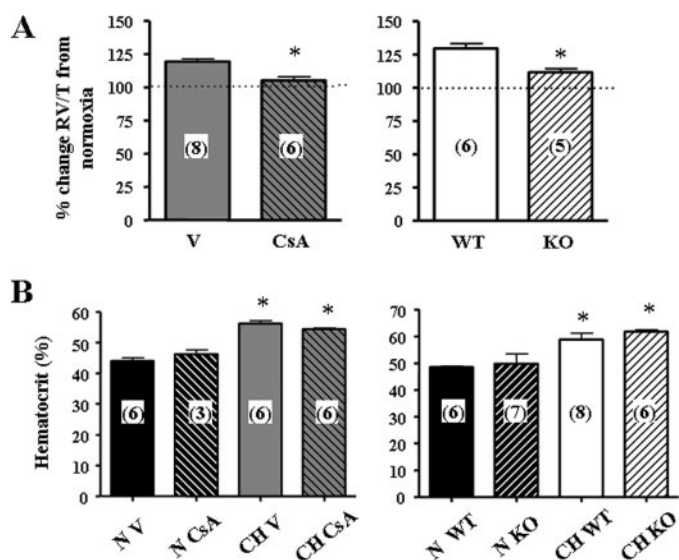


FIGURE 4. Calcineurin/NFATc3 mediates CH-induced RV hypertrophy but not polycythemia. *A*, percent change in RV/T in vehicle (V)- and CsA-treated and WT and KO mice exposed to 7 and 21 days of CH, respectively, normalized to normoxia (N) values. *, $p < 0.01$ versus V or WT. $n =$ see columns. *B*, hematocrit (%) in vehicle (V)- and CsA-treated and WT and KO mice exposed to 7 and 21 days of CH, respectively, normalized to normoxia (N) values. *, $p < 0.01$ versus N, $n =$ see columns.

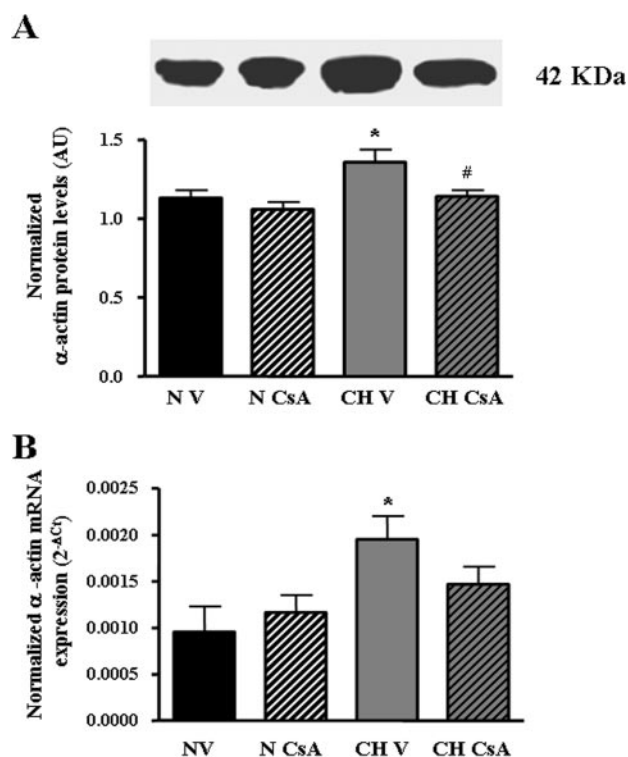


FIGURE 5. Calcineurin/NFAT mediates CH-induced up-regulation of SM- α -actin in pulmonary arteries. *A*, Western blot analysis of SM- α -actin protein expression in isolated pulmonary arteries from C57B6 mice treated with vehicle (V) or CsA and exposed to normoxia (N) or CH for 7 days. SM- α -actin band densities were normalized to total protein loaded per lane as determined by Coomassie Blue or Sypro Red II staining of the membrane. AU, arbitrary units. *, $p < 0.05$ versus N V; #, $p < 0.05$ versus CH V, $n = 6$ animals. *B*, summary of qRT-PCR analysis of SM- α -actin transcript expression in isolated pulmonary arteries from the same animals described in *A*. Threshold crossing value (C_t) was calculated using well factor background subtraction, and gene expression normalized to 18 S for each sample. *, $p < 0.05$ versus N V, $n = 5$ animals.

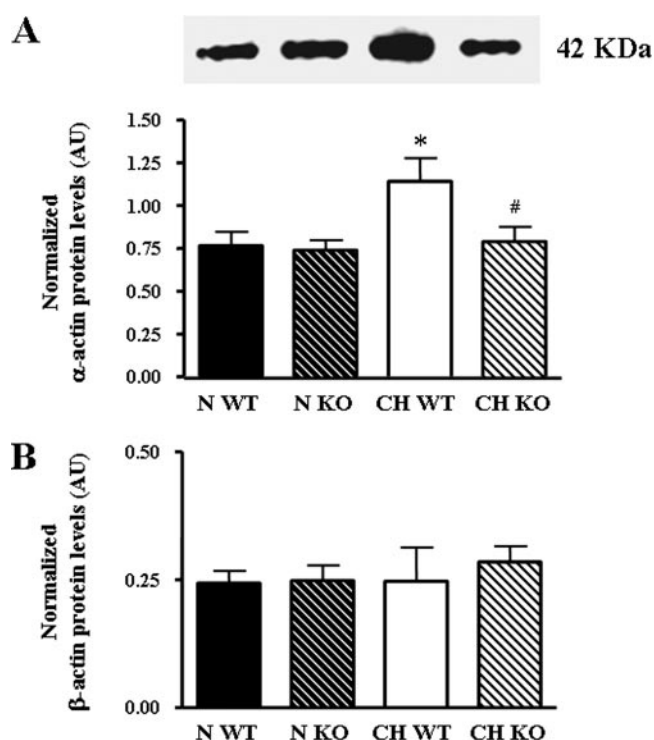


FIGURE 6. NFATc3 mediates CH-induced up-regulation of SM- α -actin in pulmonary arteries. *A*, Western blot analysis of SM- α -actin protein expression in isolated pulmonary arteries from WT and NFATc3 KO mice exposed to normoxia (N) or CH for 21 days. SM- α -actin band densities were normalized to total protein loaded per lane as determined by Coomassie Blue or Sypro Red II staining of the membrane. AU, arbitrary units. *, $p < 0.05$ versus N WT; #, $p < 0.05$ versus CH WT, $n = 4$ animals. *B*, Western blot analysis of β -actin protein expression in isolated pulmonary arteries from the same animals described in *A*. Band densities were normalized to total protein loaded per lane as determined by Sypro Red II staining of the membrane. $n = 4$ animals.

KO mice exposed to 3 weeks CH or normoxia. The analysis was performed in arteries from 3 different diameter ranges, 70–150, 151–230, 231–310, and 311–450 μm . As previously demonstrated (49–51), arterial wall thickness increased in CH WT animals. Fig. 5, *A* and *B* show the changes in the % of arterial wall thickness for arterial size range 231–310 μm , similar results were obtained in all size ranges (data not shown). Consistent with our hypothesis, NFATc3 KO did not show increased arterial wall thickness after been exposed to CH. Together with the prevented increase in α -actin expression, these results suggest that NFATc3 is involved in the PASMCH hypertrophic response that is, in part, responsible of the arterial remodeling that underlies the development of pulmonary hypertension.

DISCUSSION

The present study examined effects of CH on NFAT activity in pulmonary arteries and determined the role of NFAT in the vascular remodeling that underlies CH-induced pulmonary hypertension.

The major findings of this study are that: 1) NFATc3 transcript and protein are present in murine pulmonary arteries; 2) CH induces an increase in NFAT activity, and this activation is impaired in pulmonary arteries from NFAT-luc/NFATc3 KO mice; 3) NFAT activation is followed by an increase in NFATc3 nuclear accumulation in PASMCH; 4) pharmacological inhibi-

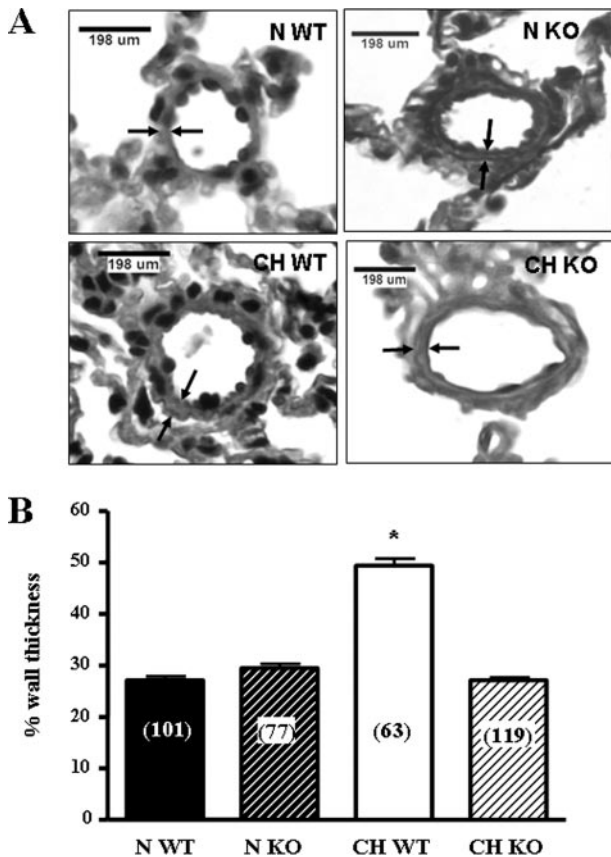


FIGURE 7. NFATc3 mediates CH-induced increases in pulmonary arterial wall thickness. *A*, representative cross sections from normoxic (*N*) and CH (21 days) WT and KO mice. Arrows point internal and external elastic laminae. *B*, percent arterial wall thickness of arteries with diameter of 231–310 μ m. *, $p < 0.001$. Arteries $n =$ see columns, number of mice: 3–4.

tion of calcineurin/NFAT pathway or genetic deletion of NFATc3 significantly attenuated CH-induced RV hypertrophy, up-regulation of SM- α -actin and increased pulmonary arterial wall thickness. These findings suggest that NFATc3 is involved in the mechanisms that lead to pulmonary hypertension during CH.

NFATc3 Is Expressed in PASMC—NFATc3 has been previously suggested to play a major role in SM contractile phenotype maintenance through the regulation of the expression of contractile proteins and potassium channels (24, 29, 52). Therefore, we first investigated if the NFATc3 isoform is expressed in murine pulmonary arteries. Indeed, NFATc3 transcript and protein were detected in isolated intrapulmonary arteries from all the mouse strains used in this study. Interestingly, Yaghi *et al.* (53) recently found that only the NFATc4 isoform is expressed in rat pulmonary arteries. However, extensive studies of the cerebral vasculature also revealed the presence of NFATc3 and c4, but not NFATc1 or c2 (23, 31, 32, 54). In contrast, NFATc1, c2, and/or c3 have been described in thoracic aortic smooth muscle cells from both rats and humans (21, 55). Recently, NFATc1, c3, and c4 were described in human myometrial arteries, no c2 was detected (56). Thus, NFAT isoform expression in VSMC appears to be somewhat species- and vascular bed-specific but this study clearly shows expression of the NFATc3 isoform in mouse PASM

CH Induces NFATc3 Activation in Pulmonary Arteries—This study provides evidence for a novel mechanism of NFATc3 activation. Our results demonstrate that CH increases NFAT activity and this activation is prevented in arteries from NFAT-luc/NFATc3 KO. In addition, CH increases NFATc3 nuclear accumulation in PASM

C. However, the time course of NFAT activation and NFATc3 accumulation are slightly different. NFAT activity was maximal at day 2 whereas NFATc3 was maximally accumulated in the nucleus of PASM

C at day 7. It is possible that other NFAT cofactors, such as AP-1 or GATA that are up-regulated by CH (57, 58), are increasing more at day 2, thus enhancing NFATc3 binding to the DNA. Also, it is possible that other NFAT isoforms expressed in PASM

C contribute to the highest NFAT activity observed at day 2 of hypoxia exposure since the activity assay is not isoform specific. However, this possibility is unlikely based on the results demonstrating that NFAT activation is dramatically impaired in arteries from NFAT-luc/NFATc3 KO mice. Our data further suggest that hypoxic activation of NFATc3 is mediated by Ca^{2+} /calcineurin because CsA prevented CH-induced NFATc3 nuclear accumulation. These results are consistent with the reported increase in PASM

C $[Ca^{2+}]_i$ during CH (3–8). Exposure to hypoxia causes hypoxic vasoconstriction due to acute inhibition of O_2 -sensing voltage-dependent K channels (K_V channels) (3). Hypoxic inhibition of K_V channels causes PASM

NFATc3 Regulates α -Actin Expression

gesting they develop pulmonary hypertension. In addition, they are also polycythemic in response to CH. Interestingly, calcineurin inhibition with CsA and the genetic deletion of NFATc3 significantly attenuated the development of RV hypertrophy without affecting the polycythemic response. These results are consistent with a recent report showing that CsA prevents CH-induced RV hypertrophy in rats (72). In this study, polycythemia was also prevented and the up-regulation of hypoxia inducible factor 1 (HIF-1)-mediated genes. Surprisingly the authors did not address whether NFAT inhibition was involved in the effects of CsA.

In addition, a few clinical studies reported that CsA improves pulmonary function of patients with primary pulmonary hypertension (73, 74) further supporting our findings.

Calcineurin/NFATc3 Mediates CH-induced Up-regulation of SM- α -actin in Pulmonary Arteries—CH-induced pulmonary hypertension is caused by increased pulmonary arterial vasoconstriction and remodeling. It has been previously shown that pulmonary arterial α -actin and myosin heavy chain expression increase after exposure to CH (2, 33, 34). In agreement with these previous findings, we have found that SM- α -actin transcript, and protein levels significantly increased after CH exposure. Interestingly, NFAT inhibition with CsA completely prevented this response. Furthermore, SM- α -actin protein levels increased in pulmonary arteries from CH WT but not from CH NFATc3 KO mice. These results are consistent with the expression of this isoform in pulmonary arteries and the reported regulation of α -actin expression by NFATc3 (21, 24). In addition, because calcineurin can dephosphorylate other cellular proteins (19), the results obtained with the NFATc3 KO confirm that the effect of CsA was specific for NFAT.

The present study demonstrates a novel effect of CH to upregulate SM- α -actin through a calcineurin/NFATc3-dependent pathway. In support of the selective regulation of SM- α -actin expression by NFATc3, no changes were observed in β -actin protein levels. These results suggest that NFATc3 is involved in PASM C hypertrophy which underlies pulmonary arterial remodeling.

It is interesting that NFATc3-mediated CH-induced increase in SM- α -actin expression does not coincide with the maximum NFAT activity at day 2 but rather overlaps with the intermediate level of activation at days 7 and 21. Therefore, it is possible that the expression of other genes that increase or decrease during CH may be transcriptionally regulated by NFATc3. For example, $K_{v}2.1$ has been shown to be downregulated by activated NFATc3 in mouse cerebral arteries smooth muscle (29) and interestingly, it is also downregulated after 2 days of CH (8, 75).

NFATc3 Mediates CH-induced Pulmonary Arterial Remodeling—Medial thickening caused in part by PASM C hypertrophy is one of the prominent features of vascular remodeling induced by CH (reviewed in Ref. 1). Our studies demonstrate pulmonary arterial remodeling (increased wall thickness) in mice after CH. NFATc3 contributes to that process evidenced by the lack of remodeling in NFATc3 KO after been exposed to CH. These results are also in agreement with the prevented up-regulation of SM- α -actin, fur-

ther supporting a role for NFATc3 in the development of pulmonary hypertension.

Differentiation of adventitial fibroblasts into myofibroblasts also contributes to medial thickening (13), a process dependent on increased expression of contractile proteins (differentiation markers) such as α -actin. Further studies are needed to determine whether the NFATc3-mediated CH-induced increase in α -actin is due to a) PASM C hypertrophy which requires increased contractile protein expression and/or b) increased myofibroblasts in the medial layer which express α -actin.

In summary, our results for the first time demonstrate that NFATc3 is expressed in PASM C and is activated by CH in a calcineurin-dependent manner. Most importantly, CH-induced RV hypertrophy, up-regulation of SM- α -actin and vascular remodeling are mediated by calcineurin/NFATc3. These findings strongly suggest that NFATc3 may be involved in the vascular changes that underlie the development of pulmonary hypertension.

Acknowledgments—We thank Dr. Laurie Glimcher for giving us the NFATc3 KO mice. We would also like to thank Dr. Molkentin for providing the 9xNFAT-luciferase mice. We thank Tamara Howard for her contribution in the vascular morphometric studies. In addition, we thank Drs. Nancy Kanagy, Thomas Resta, and Jessica Filosa for helpful discussions.

REFERENCES

- Hopkins, N., and McLoughlin, P. (2002) *J. Anat.* **201**, 335–348
- Rabinovitch, M., Gamble, W., Nadas, A. S., Miettinen, O. S., and Reid, L. (1979) *Am. J. Physiol. Heart Circ. Physiol.* **236**, H818–H827
- Weir, E. K., and Archer, S. L. (1995) *FASEB. J.* **9**, 183–189
- Li, K. X., Fouty, B., McMurtry, I. F., and Rodman, D. M. (1999) *Am. J. Physiol. Heart Circ. Physiol.* **277**, H363–H370
- Yuan, J. X.-J., Aldinger, A. M., Juhaszova, M., Wang, J., Conte, J. V., Jr., Gaine, S. P., Orens, J. B., and Rubin, L. J. (1998) *Circulation* **98**, 1400–1406
- Yu, Y., Fantozzi, I., Remillard, C. V., Landsberg, J. W., Kunichika, N., Platoshyn, O., Tigno, D. D., Thistlethwaite, P. A., Rubin, L. J., and Yuan, J. X. J. (2004) *Proc. Natl. Acad. Sci. U. S. A.* **101**, 13861–13866
- Lin, M. J., Leung, G. P. H., Zhang, W. M., Yang, X. R., Yip, K. P., Tse, C. M., and Sham, J. S. K. (2004) *Circ. Res.* **95**, 496–505
- Wang, J., Juhaszova, M., Rubin, L. J., and Yuan, X. J. (1997) *J. Clin. Investig.* **100**, 2347–2353
- Jernigan, N. L., Walker, B. R., and Resta, T. C. (2004) *Am. J. Physiol.* **287**, L1220–L1229
- Nagaoka, T., Gebb, S. A., Karoor, V., Homma, N., Morris, K. G., McMurtry, I. F., and Oka, M. (2006) *J. Appl. Physiol.* **100**, 996–1002
- Abe, K., Shimokawa, H., Morikawa, K., Uwatoku, T., Oi, K., Matsumoto, Y., Hattori, T., Nakashima, Y., Kaibuchi, K., Sueishi, K., and Takeshit, A. (2004) *Circ. Res.* **94**, 385–393
- Fagan, K. A., Oka, M., Bauer, N. R., Gebb, S. A., Ivy, D. D., Morris, K. G., and McMurtry, I. F. (2004) *Am. J. Physiol. Lung Cell Mol. Physiol.* **287**, L656–L664
- Short, M., Nemenoff, R. A., Zawada, W. M., Stenmark, K. R., and Das, M. (2004) *Am. J. Physiol. Cell Physiol.* **286**, C416–C425
- Owens, G. K. (1995) *Physiol. Rev.* **75**, 487–517
- Owens, G. K., Vernon, S. M., and Madsen, C. S. (1996) *J. Hypertens. Suppl.* **14**, S55–S64
- Owens, G. K. (1998) *Acta. Physiol. Scand.* **164**, 623–635
- Owens, G. K., Kumar, M. S., and Wamhoff, B. R. (2004) *Physiol. Rev.* **84**, 767–801
- Emmel, E. A., Verweij, C. L., Durand, D. B., Higgins, K. M., Lacy, E., and Crabtree, G. R. (1989) *Science* **246**, 1617–1620
- Rao, A., Luo, C., and Hogan, P. G. (1997) *Annu. Rev. Immunol.* **15**,

- 707–747
20. Graef, I. A., Chen, F., and Crabtree, G. R. (2001) *Curr. Opin. Genet. Dev.* **11**, 505–512
 21. Wada, H., Hasegawa, K., Morimoto, T., Kakita, T., Yanazume, T., Abe, M., and Sasayama, S. (2002) *J. Cell Biol.* **156**, 983–991
 22. Ohkawa, Y., Hayashi, K., and Sobue, K. (2003) *Biochem. Biophys. Res. Commun.* **301**, 78–83
 23. Gonzalez Bosc, L. V., Wilkerson, M. K., Bradley, K. N., Eckman, D. M., Hill-Eubanks, D. C., and Nelson, M. T. (2004) *J. Biol. Chem.* **279**, 10702–10709
 24. Gonzalez Bosc, L. V., Layne, J., Nelson, M. T., and Hill-Eubanks, D. C. (2004) *J. Biol. Chem.* **280**, 26113–26120
 25. Graef, I. A., Chen, F., Chen, L., Kuo, A., and Crabtree, G. R. (2001) *Cell* **105**, 863–875
 26. Fatigati, V., and Murphy, R. A. (1984) *J. Biol. Chem.* **259**, 14383–14388
 27. Hill-Eubanks, D. C., Gomez, M. F., Stevenson, A. S., and Nelson, M. T. (2003) *Trends Cardiovasc. Med.* **13**, 56–62
 28. Hogan, P. G., Chen, L., Nardone, J., and Rao, A. (2003) *Genes Dev.* **17**, 2205–2232
 29. Amberg, G. C., Rossow, C. F., Navedo, M. F., and Santana, L. F. (2004) *J. Biol. Chem.* M408789200
 30. Abbott, K. L., Loss, J. R., Robida, A. M., and Murphy, T. J. (2000) *Mol. Pharmacol.* **58**, 946–953
 31. Gomez, M. F., Stevenson, A. S., Bonev, A. D., Hill-Eubanks, D. C., and Nelson, M. T. (2002) *J. Biol. Chem.* **277**, 37756–37764
 32. Stevenson, A. S., Gomez, M. F., Hill-Eubanks, D. C., and Nelson, M. T. (2001) *J. Biol. Chem.* **276**, 15018–15024
 33. Durmowicz, A. G., and Stenmark, K. R. (1999) *Pediatr. Res.* **20**, e91–e102
 34. Jones, R., Jacobson, M., and Steudel, W. (1999) *Am. J. Resp. Cell Mol. Biol.* **20**, 582–594
 35. Owens, G. K., Rabinovitch, P. S., and Schwartz, S. M. (1981) *Proc. Natl. Acad. Sci. U. S. A.* **78**, 7759–7763
 36. Chassagne, C., Eddahibi, S., Adamy, C., Rideau, D., Marotte, F., Dubois-Rande, J. L., Adnot, S., Samuel, J. L., and Teiger, E. (2000) *Am. J. Resp. Cell Mol. Biol.* **22**, 323–332
 37. Morrell, N. W., Atochina, E. N., Morris, K. G., Danilov, S. M., and Stenmark, K. R. (1995) *J. Clin. Investig.* **96**, 1823–1833
 38. Orte, C., Polak, J. M., Haworth, S. G., Yacoub, M. H., and Morrell, N. W. (2000) *J. Pathol.* **192**, 379–384
 39. Hautmann, M. B., Thompson, M. M., Swartz, E. A., Olson, E. N., and Owens, G. K. (1997) *Circ. Res.* **81**, 600–610
 40. Braz, J. C., Bueno, O. F., Liang, Q., Wilkins, B. J., Dai, Y. S., Parsons, S., Braunwart, J., Glascock, B. J., Klevitsky, R., Kimball, T. F., Hewett, T. E., and Molkentin, J. D. (2003) *J. Clin. Investig.* **111**, 1475–1486
 41. Oukka, M., Ho, I. C., de la Brousse, F. C., Hoey, T., Grusby, M. J., and Glimcher, L. H. (1998) *Immunity* **9**, 295–304
 42. Wilkins, B. J., De Windt, L. J., Bueno, O. F., Braz, J. C., Glascock, B. J., Kimball, T. F., and Molkentin, J. D. (2002) *Mol. Cell Biol.* **22**, 7603–7613
 43. Resta, T. C., Gonzales, R. J., Dail, W. G., Sanders, T. C., and Walker, B. R. (1997) *Am. J. Physiol. Heart Circ. Physiol.* **272**, H806–H813
 44. Resta, T. C., Chicoine, L. G., Omdahl, J. L., and Walker, B. R. (1999) *Am. J. Physiol. Heart Circ. Physiol.* **276**, H699–H708
 45. Meyrick, B., and Reid, L. (1979) *Anat. Rec.* **193**, 71–97
 46. Livak, K. J., and Schmittgen, T. D. (2001) *Methods* **25**, 402–408
 47. Ferri, C., Bellini, C., De Angelis, C., De Siatì, L., Perrone, A., Properzi, G., and Santucci, A. (1995) *J. Clin. Pathol.* **48**, 519–524
 48. Yang, X., Chen, W., and Chen, J. (1997) *Chin. Med. J. (Engl.)* **110**, 104–108
 49. Dumitrascu, R., Weissmann, N., Ghofrani, H. A., Dony, E., Beuerlein, K., Schmidt, H., Stasch, J. P., Gnoth, M. J., Seeger, W., Grimminger, F., and Schermuly, R. T. (2006) *Circulation* **113**, 286–295
 50. Paddenberg, R., Stieger, P., von Lilien, A. L., Faulhammer, P., Goldenberg, A., Tillmanns, H. H., Kummer, W., and Braun-Dullaeus, R. C. (2007) *Respir Res.* **8**:15, 15
 51. Resta, T., Sanders, T., Eichinger, M., Crowley, M., and Walker, B. (1998) *Resp. Physiol.* **114**, 161–173
 52. Nieves-Cintrón, M., Amberg, G. C., Nichols, C. B., Molkentin, J. D., and Santana, L. F. (2007) *J. Biol. Chem.* **282**, 3231–3240
 53. Yaghi, A., and Sims, S. M. (2005) *Am. J. Physiol. Lung Cell Mol. Physiol.* **289**, L1061–L1074
 54. Gomez, M. F., Gonzalez Bosc, L. V., Stevenson, A. S., Wilkerson, M. K., Hill-Eubanks, D. C., and Nelson, M. T. (2003) *J. Biol. Chem.* **278**, 46847–46853
 55. Boss, V., Abbott, K. L., Wang, X. F., Pavlath, G. K., and Murphy, T. J. (1998) *J. Biol. Chem.* **273**, 19664–19671
 56. Nilsson, L. M., Sun, Z. W., Nilsson, J., Nordstrom, I., Chen, Y. W., Molkentin, J. D., Wide-Swensson, D., Hellstrand, P., Lydrup, M. L., and Gomez, M. F. (2007) *Am. J. Physiol. Cell Physiol.* **292**, C1167–C1178
 57. Semenza, G. L. (1999) *Cell* **98**, 281–284
 58. Kallio, P. J., Okamoto, K., O'Brien, S., Carrero, P., Makino, Y., Tanaka, H., and Poellinger, L. (1998) *EMBO J.* **17**, 6573–6586
 59. Wang, J., Weigand, L., Lu, W., Sylvester, J. T., Semenza, L., and Shimoda, L. A. (2006) *Circ. Res.* **98**, 1528–1537
 60. Nakayama, H., Wilkin, B. J., Bodi, I., and Molkentin, J. D. (2006) *FASEB J.* **20**, 1660–1670
 61. Rosenberg, P., Hawkins, A., Stiber, J., Shelton, J. M., Hutcheson, K., Bassel-Duby, R., Shin, D. M., Yan, Z., and Williams, R. S. (2004) *Proc. Natl. Acad. Sci. U. S. A.* **101**, 9387–9392
 62. Naik, J. S., Earley, S., Resta, T. C., and Walker, B. R. (2005) *J. Appl. Physiol.* **98**, 1119–1124
 63. Ip, S. P., Chan, Y. W., and Leung, P. S. (2002) *Pancreas* **25**, 296–300
 64. Shimoda, L. A., Sham, J. S., and Sylvester, J. T. (2000) *Physiol. Res.* **49**, 549–560
 65. Blumberg, F. C., Wolf, K., Arzt, M., Lorenz, C., Riegger, G. A. J., and Pfeifer, M. (2003) *J. Appl. Physiol.* **94**, 446–452
 66. El Gamal, Y., Hossny, E., Awwad, K., Mabrouk, R., and Boseila, N. (2002) *Ann. Allergy Asthma Immunol.* **88**, 370–373
 67. Ivy, D. D., Le Cras, T. D., Horan, M. P., and Abman, S. H. (1998) *Am. J. Physiol.* **274**, L535–L541
 68. Nishida, M., Eshiro, K., Okada, Y., Takaoka, M., and Matsumura, Y. (2004) *J. Cardiovasc. Pharmacol.* **44**, 187–191
 69. Soma, S., Takahashi, H., Muramatsu, M., Oka, M., and Fukuchi, Y. (1999) *Am. J. Resp. Cell Mol. Biol.* **20**, 620–630
 70. Yuyama, H., Fujimori, A., Sanagi, M., Koakutsu, A., Noguchi, Y., Sudoh, K., Sasamata, M., and Miyata, K. (2005) *Vasc. Pharmacol.* **43**, 40–46
 71. Cheever, K. H. (2005) *J. Cardiovasc. Nurs.* **20**, 108–116
 72. Koulmann, N., Novel-Chate, V., Peinnequin, A., Chapot, R., Serrurier, B., Simler, N., Richard, H., Ventura-Clapier, R., and Bigard, X. (2006) *Am. J. Respir. Crit. Care Med.* **174**, 699–705
 73. Morelli, S., Giordano, M., De Marzio, P., Priori, R., Sgreccia, A., and Valesini, G. (1993) *Lupus* **2**, 367–369
 74. Padeh, S., Laxer, R. M., Silver, M. M., and Silverman, E. D. (1991) *Arthritis Rheum.* **34**, 1575–1579
 75. Shimoda, L. A., Manalo, D. J., Sham, J. S. K., Semenza, G. L., and Sylvester, J. T. (2001) *Am. J. Physiol. Lung Cell Mol. Physiol.* **281**, L202–L208